

This article was downloaded by:

On: 22 January 2011

Access details: *Access Details: Free Access*

Publisher *Taylor & Francis*

Informa Ltd Registered in England and Wales Registered Number: 1072954 Registered office: Mortimer House, 37-41 Mortimer Street, London W1T 3JH, UK



## The Journal of Adhesion

Publication details, including instructions for authors and subscription information:

<http://www.informaworld.com/smpp/title~content=t713453635>

### Strength Loss Mechanisms for Adhesive Bonds to Electroplated Zinc and Cold Rolled Steel Substrates Subjected to Moist Environments

Robert T. Foister<sup>a</sup>; Sandra L. F. Niks<sup>a</sup>; Michael J. Barker<sup>a</sup>

<sup>a</sup> Polymers Department, General Motors Research Laboratories, Warren, Michigan, U.S.A.

**To cite this Article** Foister, Robert T. , Niks, Sandra L. F. and Barker, Michael J.(1989) 'Strength Loss Mechanisms for Adhesive Bonds to Electroplated Zinc and Cold Rolled Steel Substrates Subjected to Moist Environments', *The Journal of Adhesion*, 30: 1, 105 – 118

**To link to this Article:** DOI: 10.1080/00218468908048200

**URL:** <http://dx.doi.org/10.1080/00218468908048200>

PLEASE SCROLL DOWN FOR ARTICLE

Full terms and conditions of use: <http://www.informaworld.com/terms-and-conditions-of-access.pdf>

This article may be used for research, teaching and private study purposes. Any substantial or systematic reproduction, re-distribution, re-selling, loan or sub-licensing, systematic supply or distribution in any form to anyone is expressly forbidden.

The publisher does not give any warranty express or implied or make any representation that the contents will be complete or accurate or up to date. The accuracy of any instructions, formulae and drug doses should be independently verified with primary sources. The publisher shall not be liable for any loss, actions, claims, proceedings, demand or costs or damages whatsoever or howsoever caused arising directly or indirectly in connection with or arising out of the use of this material.

*J. Adhesion*, 1989, Vol. 30, pp. 105–118  
Reprints available directly from the publisher  
Photocopying permitted by license only  
© 1989 Gordon and Breach Science Publishers, Inc.  
Printed in the United Kingdom

# Strength Loss Mechanisms for Adhesive Bonds to Electroplated Zinc and Cold Rolled Steel Substrates Subjected to Moist Environments

ROBERT T. FOISTER, SANDRA L. F. NIKS and MICHAEL J. BARKER

*Polymers Department, General Motors Research Laboratories, Warren, Michigan 48090-9055, U.S.A.*

*(Received December 24, 1988; in final form April 7, 1989)*

Mechanisms of strength loss which affect the durability of epoxy adhesive bonds in moist environments were investigated for electroplated zinc and cold rolled steel substrates. Activation energies for adhesion loss, formation of corrosion product on the substrate surface, and moisture diffusion in the adhesive were determined experimentally. For cold rolled steel substrates, the activation energy for adhesion loss was identical, within experimental error, to the measured activation energy for moisture diffusion in the adhesive. Both of these values were substantially less ( $\approx 40\%$ ) than the activation energy for formation of corrosion product. This confirms the previous results of Gledhill and Kinloch (*J. Adhesion* **6**, 315 (1974)), who attributed strength loss to thermodynamic instability of the adhesive/substrate interface due to the presence of moisture. In contrast, for electroplated zinc substrates, activation energies for adhesion loss and corrosion product formation were essentially equal, and were both significantly higher than that for moisture diffusion. Consequently, it was concluded that corrosion of the electroplated zinc layer was responsible for bond strength loss. Formation of corrosion product in the bond was not, therefore, a post-failure phenomenon as was the case for cold rolled steel.

**KEY WORDS** Structural adhesives; environmental durability; galvanized substrates; lap shear strength; corrosion; failure mechanisms.

## INTRODUCTION

The increased use of zinc-coated steel in automotive applications has been motivated primarily by efforts to improve corrosion protection in typical service environments. While the presence of a sacrificial zinc layer does offer a degree of enhanced corrosion protection, successful incorporation of zinc-coated steels into automotive production requires compatibility with processes such as painting and joining, if the full advantages of these materials are to be derived.

Depending on the particular application, both welding and adhesive bonding have been used to join zinc-coated steels. These processes have not been entirely

free of difficulties, however. Some of these difficulties, like weld tip maintenance and selectivity of adhesive materials for particular types of coated steel, had been anticipated based on experience with other metallic substrates, primarily cold rolled steel. In the area of adhesive bonding, however, additional problems such as the influence of surface morphology and chemical heterogeneity on adhesive bond strength and durability, have only emerged as a result of systematic investigations using particular materials.<sup>1,2</sup> For example, by evaluating the performance of various epoxy adhesives bonded to different types of zinc-coated steels, it was shown that unaged bond strength was greater for electroplated zinc substrates, which had considerable surface roughness, than for relatively smooth "hot dipped" zinc-coated substrates.<sup>1</sup> Likewise, durability of bonds to zinc-coated steels was found to depend on the degree of chemical heterogeneity in the oxide layer of the substrate.<sup>2</sup>

Perhaps the most significant conclusion of work carried out thus far in the adhesive bonding of zinc-coated steels is that the environmental durability of bonded joints is intimately related to the corrosion of the substrate. This has been confirmed by numerous authors.<sup>1-5</sup> For electroplated substrates Arnold<sup>4</sup> has shown that retention of initial bond strength in a cyclic moisture, salt water immersion environment is proportional to zinc coating weight. Also, Maedo, *et al.*<sup>5</sup> have suggested that trace elements other than zinc in the oxide layer of hot dipped substrates actually enhance interfacial corrosion (and thereby accelerate the loss of adhesive bond strength) compared with the zinc oxides typically found on electroplated zinc substrates.

However, there is still a very important question which has not been answered, and this is whether substrate corrosion *initiates* bond failure, or whether corrosion is a *post-failure* phenomenon. This is not just of passing interest—the answer to this question will determine the approach to take to maximize bond durability. If diffusion of water into the adhesive is the rate limiting process, retardation of this process (by choosing adhesives which have low moisture diffusivities, for example) will increase bond durability. However, if bond strength loss is coincident with substrate corrosion, then the proper strategy to increase durability is to retard corrosion initiation by protecting bond edges with an appropriate conversion coating (e.g., zinc phosphate), together with an electro-deposition primer. It is, therefore, the main purpose of this work to determine the mechanism of strength loss in moist environments for bonds to zinc-coated steel substrates.

For epoxy adhesive bonds to cold rolled steel, Gledhill and Kinloch<sup>6</sup> have shown that magnetite ( $\text{Fe}_3\text{O}_4$ ) forms on the failure surfaces of bonds exposed to a moist environment. Furthermore, they found that the activation energy of adhesion loss in a moist environment was comparable to the activation energy for moisture diffusion in typical epoxy adhesives. Formation of the corrosion product, however, occurred with an activation energy significantly higher than that measured for adhesion loss. Thus, for bonds to cold rolled steel, it was argued that corrosion occurred after loss of adhesion between the adhesive and the substrate, the loss of adhesion being due to thermodynamic instability of the adhesive/substrate interface to the presence of moisture.

Following the approach of Gledhill and Kinloch,<sup>6</sup> we have measured activation energies for model adhesive bonds to electroplated zinc substrates, and for the same adhesive bonded to cold rolled steel. In separate experiments we also measured the activation energy for the diffusion of water into the adhesive which was used to bond these materials. By assuming that diffusion of moisture into the adhesive joint is accurately modeled by the diffusivity which is measured in the sorption experiments, a straightforward comparison of the various activation energies provides the basis for establishing probable mechanism of adhesion loss in moist environments for these two important substrates.

## EXPERIMENTAL

### Materials

*Substrates* Sheet steel (Republic Steel, Inc.) with an 8.7  $\mu\text{m}$  layer of electroplated zinc which had a coating weight of 0.18  $\text{kg m}^{-2}$ , as well as 1010 cold rolled steel, were used as substrates. The thickness of the electroplated zinc substrate was 1.1 mm, while that of the cold rolled steel was 2.7 mm. Standard single lap shear coupons, 25.4  $\times$  101.6 mm, were prepared in accordance with ASTM D1002. The cold rolled steel samples were grit blasted with a suspension of 200 mesh silica in water at 500 kPa, and cleaned with acetone prior to bonding. The electroplated zinc samples were cleaned with trichloroethane and acetone prior to bonding.

*Adhesive* An unfilled, two-part epoxy adhesive was used to bond both substrates. This adhesive was a mixture of 100 phr D.E.N. 431 epoxy novolac (Dow Chemical), 50 phr Epirez 5048 (Interez, Inc.), and was catalyzed by 9.5 phr AP5 (1-(2-hydroxypropyl)-2-methylimidazole from Archem, Inc.). The fully-cured adhesive, which has been extensively investigated in other contexts,<sup>7,8</sup> has a glass transition temperature (measured by differential scanning calorimetry) of 143°C, and shows excellent adhesion and durability to both cold rolled and electroplated zinc substrates.<sup>1</sup>

### Adhesive sample preparation and testing

Lap shear samples were made with a 12.7 mm bond overlap and a 0.127 mm bond thickness. Bondline thickness was maintained by incorporation of a length of copper wire of the appropriate diameter into the bond prior to adhesive cure. Samples were assembled in a bonding fixture designed to give a constant 100 kPa clamping pressure. The fixture was heated to the cure temperature before lap shear assembly.

The samples were given an initial cure at 150°C for twenty-five minutes in a forced air oven. All samples were then post cured through the following cycle which simulates a typical automotive paint bake process.

- 1) 75 minutes at 160°C
- 2) Cold tap water quench

- 3) 30 minutes at 135°C
- 4) 45 minutes at room temperature
- 5) 20 minutes at 135°C
- 6) 45 minutes at room temperature
- 7) 40 minutes at 160°C.

After exposure to the appropriate environment (see below), lap shear strengths were determined by testing the samples on an Instron (Model TTC) test machine using a crosshead speed of  $1.27 \text{ mm min}^{-1}$ . Mean lap shear strengths for a particular condition (e.g., time of exposure at a given temperature) were determined from a set of five samples.

#### **Sample preparation for diffusivity determination**

Cast sheets of the adhesive were prepared in the following manner. The resin mixture was degassed at 100°C for five to six hours, maintained under vacuum over night, and then reheated to 100°C for four hours. The mixture was then cooled and the appropriate amount of imidazole catalyst added under vacuum, after which the mixture was poured into a glass plate assembly to form sheets. The glass plate assembly consisted of two mold release (Frekote 44) treated, Pyrex glass plates separated by stainless steel shims (approximately 0.85 mm thickness). A bead of silicone adhesive was used around the periphery to contain the liquid adhesive, and the assembly was held together with binder clips. Following a 24 hour gelation at room temperature, the sheets were cured for thirty minutes at 150°C, cooled to room temperature, then demolded. Rectangular samples  $32 \times 12.7 \times 0.85 \text{ mm}$  were cut from the cured sheet using a diamond saw, then were post cured through the simulated paint cycle described above.

#### **Environmental exposures**

*Adhesive samples* Lap shear samples were first dip coated in a paraffin wax (except for the actual bonded areas), then were immersed in distilled water baths maintained at constant ( $\pm 1^\circ\text{C}$ ) temperatures of 35, 45, 60, and 80°C. Periodically, sets of five samples were removed from the baths, dried, then tested within one half hour, which is much less than the characteristic time for significant loss of moisture due to diffusion. Percent strength retention as a function of exposure time at each temperature was determined with respect to samples maintained at room temperature in a desiccator.

*Diffusivity samples* Thin rectangular samples of predetermined mass were labeled for identification, then immersed in distilled water baths maintained at constant ( $\pm 1^\circ\text{C}$ ) temperatures of 30, 45, 60, 73, and 83°C. For each of four samples at the immersion temperature, percent mass gain due to moisture sorption was determined as a function of time by removing samples from the

environment, wiping with cheesecloth to remove surface moisture, then weighing with an analytical balance. Equilibrium moisture content was approximated from the horizontal portion of the % mass gain *versus* time curve for each temperature.

#### Determination of activation energies

*Adhesion loss* Fractional strength retention *versus* time data were modeled as simple exponentials. Generally this representation of the data was excellent; the correlation coefficients were in all cases better than 0.97. The rate of adhesion loss could, therefore, be approximated with a temperature-dependent constant  $k$  of the standard Arrhenius form:

$$\text{Fractional Strength Retention} \sim e^{-kt},$$

$$\text{where } k = A \exp(-E_a/RT).$$

The activation energy ( $E_a$ ) was determined from a plot of  $\ln k$  vs.  $1/T$ .

*Formation of corrosion product* For bonds to zinc-coated steels, formation of corrosion product on bond failure surfaces created a very distinct dark gray area, which began along the bond edges and extended inward. (This is discussed in more detail below.) With increasing exposure time, this dark area gradually covered the entire bond. The encroachment of this area as a function of time can be quantitatively expressed *via* the fractional decrease in non-corroded area. The non-corroded area was traced on paper for each sample of a given set (i.e., for each temperature and exposure time), and the weight of this tracing was compared with the weight of a tracing of the initial bonded area for the same sample.

As in the case of adhesion loss, the decrease in non-corroded area as a function of time can be effectively modeled as an exponential, with a rate constant which can be plotted as a function of temperature to yield the appropriate activation energy.

*Moisture diffusion in the epoxy adhesive* If it is assumed that diffusion of moisture into the adhesive is Fickian, the diffusivity can be determined from the initial slope of a percent moisture uptake versus square root of time curve.<sup>9</sup> By further assuming a temperature dependence of the Arrhenius form for the diffusivity, the activation energy for moisture diffusion can be calculated in the same manner as described above.

*Scanning Electron Microscopy* Lap shear failure surfaces were gold-coated and examined in an ISI Model DS-130 scanning electron microscope.

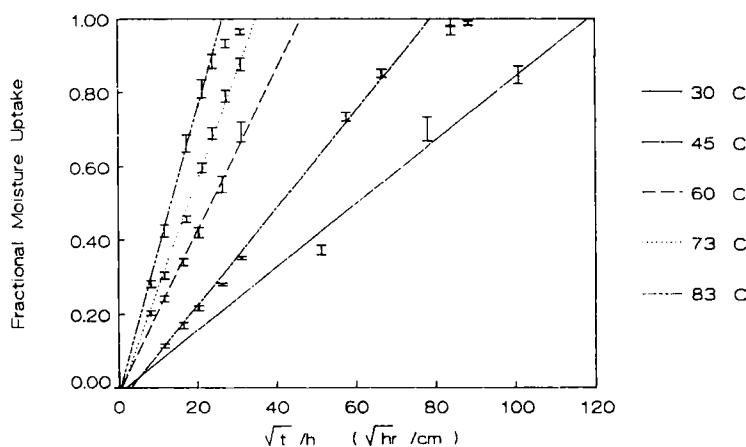


FIGURE 1 Fractional moisture uptake *versus* square root of time at five temperatures. Points shown are mean values of four samples.

## RESULTS AND DISCUSSION

### Activation energy for moisture diffusion

A plot of fractional moisture uptake *versus* the square root of time divided by  $h$ , the sample thickness, for the five immersion conditions is shown in Figure 1. With experimental variability, linearity is maintained up to at least 60% of the apparent equilibrium value for each temperature. Linear least squares fits to the data gave correlation coefficients  $\geq 0.9$ . It is also important to note that all immersion temperatures are considerably less than the "dry" glass transition temperature of the system ( $143^{\circ}\text{C}$ ), as well as the "wet," i.e., moisture-equilibrated, value of approximately  $95^{\circ}\text{C}$ .<sup>10</sup>

If we assume that the diffusion is Fickian, the diffusivity ( $D$ ) at each temperature can be determined<sup>9</sup> from

$$D = (\pi/16)(\text{slope})^2.$$

The value of the slope is calculated from the linear portion of a plot of moisture uptake *versus* the square root of time divided by sample thickness. In these plots, moisture uptake is expressed by the quantity  $[M(t) - M(0)]/[M(\infty) - M(0)]$ ,

TABLE I  
Mean values of the diffusivity and equilibrium moisture content at various temperatures

$D(10^{-9} \text{ cm}^2 \text{ sec}^{-1})$	$[M(\infty) - M(0)]/M(0) \times 100\%$	$T(^{\circ}\text{C})$
4.21 ( $\pm 0.37$ )	8.9 ( $\pm 0.1$ )	30
6.87 ( $\pm 0.16$ )	8.9 ( $\pm 0.2$ )	45
23.9 ( $\pm 1.7$ )	8.9 ( $\pm 0.1$ )	60
41.9 ( $\pm 1.7$ )	8.6 ( $\pm 0.1$ )	73
69.4 ( $\pm 5.3$ )	9.3 ( $\pm 0.1$ )	83

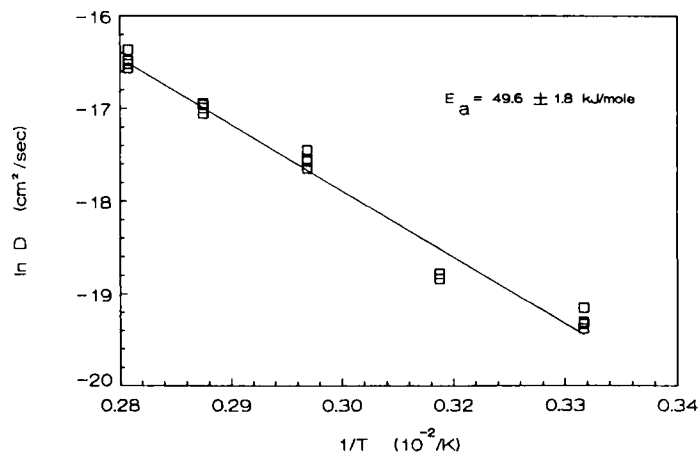


FIGURE 2 Arrhenius plot of  $\ln D$  versus reciprocal absolute temperature. Solid curve is least squares fit of all data.

where  $M(t)$  is the mass of the sample at time  $t$ ,  $M(0)$  the initial dry mass, and  $M(\infty)$  the apparent equilibrium value. Calculated mean values of  $D$  and the equilibrium moisture content (in %) at the various test temperatures are given in Table I. From these values it can be seen that  $D$  increases with temperature, as expected, but that there is little variation in the equilibrium moisture content over this temperature range.

An Arrhenius plot of  $\ln D$  versus the reciprocal absolute temperature is shown in Figure 2. Each of the points represents the calculated temperature dependence for a particular sample. The line through the points is the linear least squares fit of all the data. This gives an activation energy of  $49.6 \text{ kJ mol}^{-1}$ , with a standard

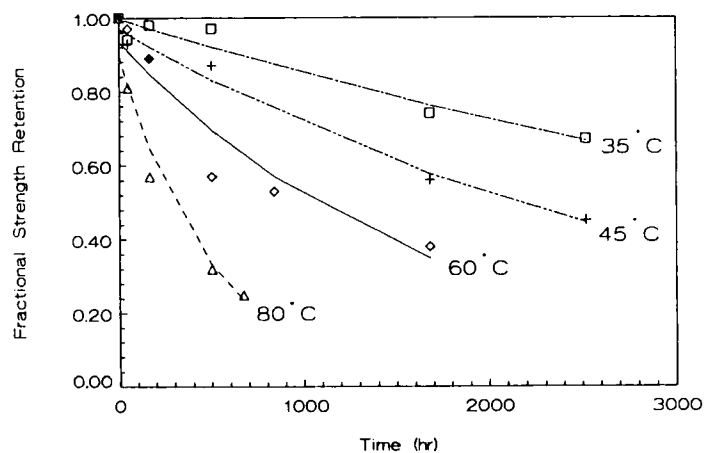


FIGURE 3 Fractional strength retention for bonds to cold rolled steel. Curves are exponential fits to the data points.



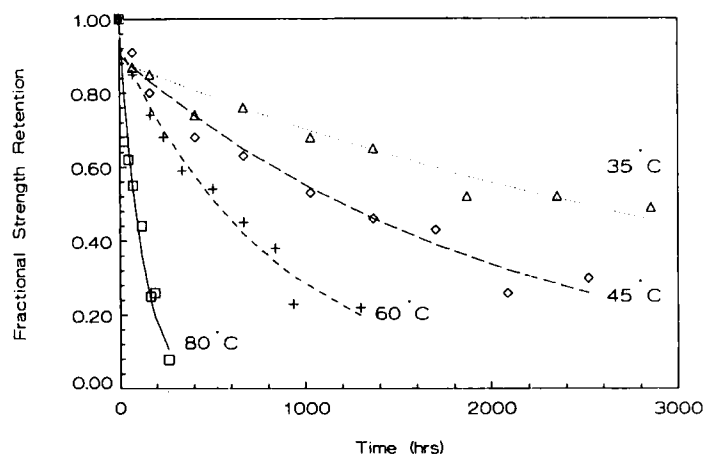


FIGURE 4 Fractional strength retention for bonds to electroplated zinc. Curves are exponential fits to the data points.

error of  $1.8 \text{ kJ mol}^{-1}$ . This value for the activation energy is somewhat higher than other selected values quoted in the literature<sup>6</sup>, and may be a reflection of the rather high crosslink density of this particular system.<sup>8</sup>

#### Activation energy for adhesion loss

As anticipated from the variation in lap shear strengths (mean initial value for electroplated zinc =  $13.0 \pm 1.5 \text{ MPa}$ , for cold rolled steel =  $21.4 \pm 1.2 \text{ MPa}$ ), there was a good deal of scatter (anywhere from 5 to 10%) in the strength retention *versus* time data shown in Figures 3 (cold rolled steel) and 4 (electroplated zinc). However, data at each temperature could be effectively modeled as a simple

TABLE II  
Rate constants ( $\text{hr}^{-1}$ ) for various processes  
as a function of temperature

<i>A. Adhesion Loss, Cold Rolled Steel</i>	
$k(80^\circ\text{C})$	$= 1.985 \times 10^{-3}$
$k(60^\circ\text{C})$	$= 5.889 \times 10^{-4}$
$k(45^\circ\text{C})$	$= 3.098 \times 10^{-4}$
$k(35^\circ\text{C})$	$= 1.603 \times 10^{-4}$
<i>B. Adhesion Loss, Electroplated Zinc</i>	
$k(80^\circ\text{C})$	$= 8.479 \times 10^{-3}$
$k(60^\circ\text{C})$	$= 1.192 \times 10^{-3}$
$k(45^\circ\text{C})$	$= 4.937 \times 10^{-4}$
$k(35^\circ\text{C})$	$= 2.325 \times 10^{-4}$
<i>C. Formation of Corrosion Product</i>	
$k(80^\circ\text{C})$	$= 1.239 \times 10^{-2}$
$k(60^\circ\text{C})$	$= 2.117 \times 10^{-3}$
$k(45^\circ\text{C})$	$= 8.981 \times 10^{-4}$
$k(35^\circ\text{C})$	$= 3.750 \times 10^{-4}$

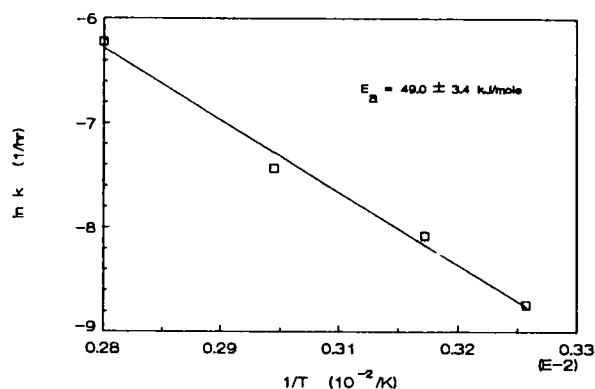


FIGURE 5A Arrhenius plot of  $\ln k$  versus reciprocal absolute temperature for adhesion loss to cold rolled steel.

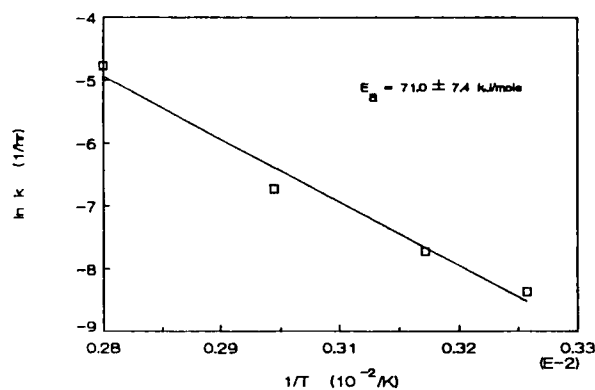


FIGURE 5B Arrhenius plot of  $\ln k$  versus reciprocal absolute temperature for adhesion loss to electroplated zinc.

exponential decay, as is shown by the solid curves in Figures 3 and 4. The calculated rate constants ( $k$ ) for each temperature are given in Table II.

For the cold rolled steel substrates, the appropriate Arrhenius plot (Figure 5) gives an activation energy for adhesion loss of  $49.0 \text{ kJ mol}^{-1}$ , with a standard error of  $3.4 \text{ kJ mol}^{-1}$ . This is essentially equal to the activation energy for moisture diffusion given above. For electroplated zinc, however, the activation energy was found to be  $71.0 \text{ kJ mol}^{-1}$  (with a standard error of  $7.4 \text{ kJ mol}^{-1}$ ), which is significantly higher than that found for either moisture diffusion, or adhesion loss for cold rolled steel.

#### Activation energy for corrosion of electroplated zinc

The formation of a corrosion product on adhesively bonded electroplated zinc substrates was, as pointed out above, quite noticeable. In fact, a clear delineation

of corroded and non-corroded areas could be made by visual inspection. The appearance of the failure surfaces after varying exposure times at 60°C is illustrated in the sequence of photographs in Figure 6.

It was also of interest to examine, on a microscopic scale, the morphology of the substrate in the corroded and non-corroded regions. Figure 7A shows a scanning electron micrograph of the non-corroded area. This surface morphology of closely packed, plate-like zinc crystals is typical of the electroplating process.<sup>2</sup> In contrast, Figure 7B shows that the corroded surface is characterized by a significantly altered morphology. This is similar to the appearance of a basic zinc chloride corrosion product on failure surfaces of samples exposed to a high humidity, salt water immersion cycle.<sup>2</sup> Although its identity was not determined in the present case, the corrosion product is probably zinc hydroxide, which forms

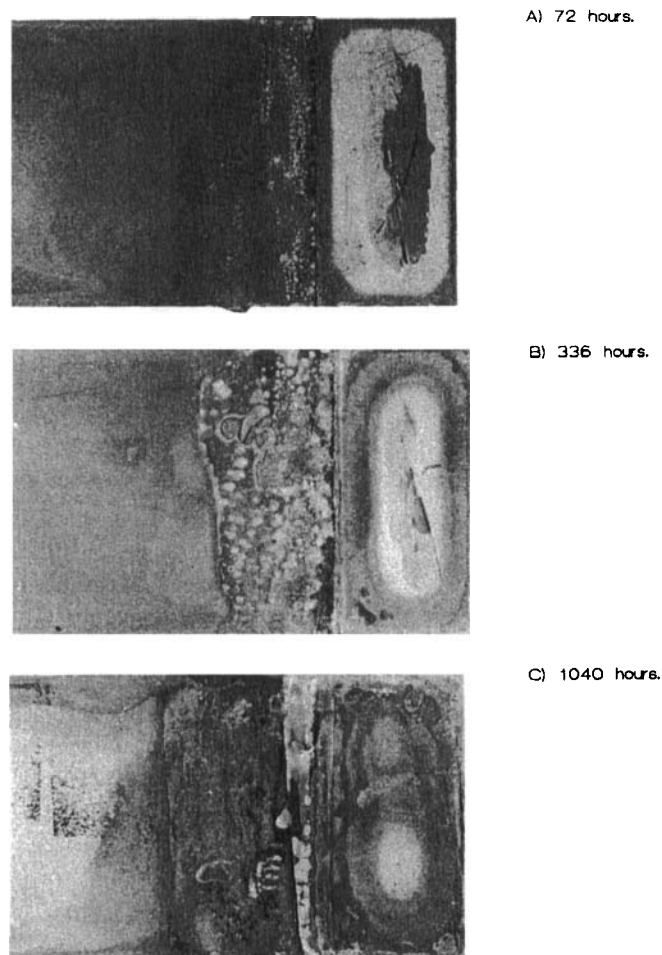
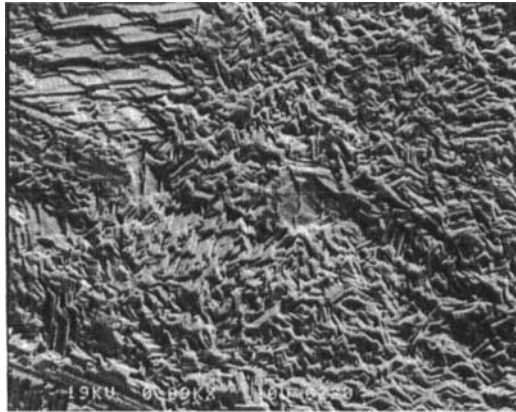


FIGURE 6 Failure surfaces of bonds to electroplated zinc showing corrosion ingress and loss of bonded area after various exposure times at 60°C.

A.



B.



FIGURE 7 A) Scanning electron micrograph of non-corroded area of electroplated zinc substrate. B) Micrograph of corroded area showing altered morphology.

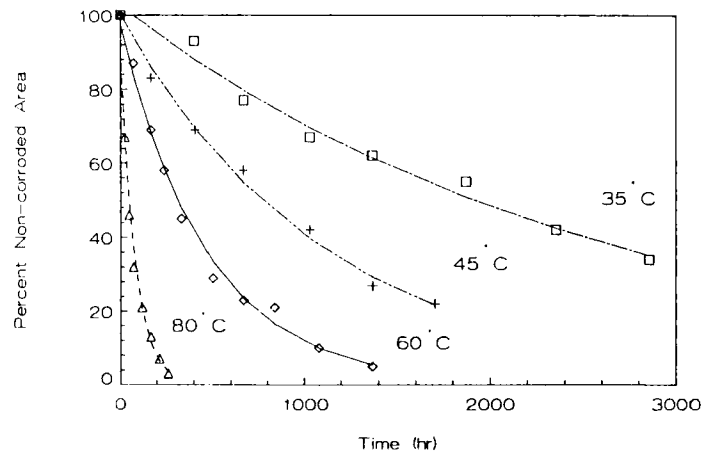


FIGURE 8 Percent non-corroded bond area *versus* time for electroplated zinc. Curves are exponential fits to the data points.

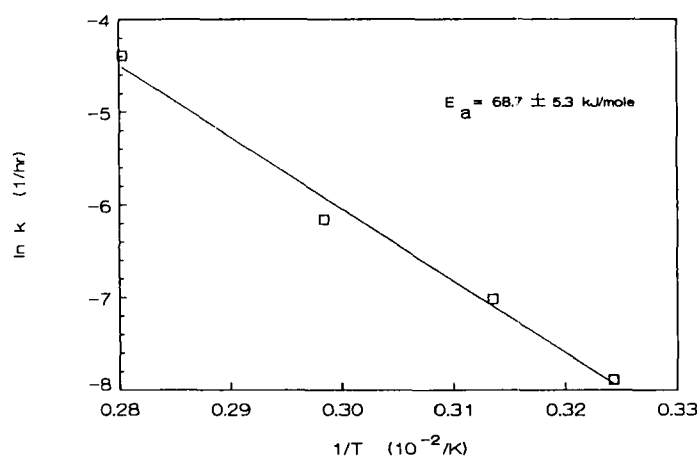


FIGURE 9 Arrhenius plot of  $\ln k$  versus  $1/T$  for formation of corrosion product on electroplated zinc.

on zinc surfaces subjected to environments (such as the adhesive bond subjected to high temperature water immersion) which are oxygen deficient.<sup>5</sup>

Figure 8 shows the measured decrease in non-corroded area as a function of time at various temperatures and Figure 9 is the corresponding Arrhenius plot for the temperature dependence of the rate constant (see Table II for individual values). This plot gives an activation energy of  $68.7 \text{ kJ mol}^{-1}$ , with a standard error of  $5.3 \text{ kJ mol}^{-1}$ . Considering the experimental uncertainties, this activation energy is essentially equivalent to the value of  $71.0 \text{ kJ mol}^{-1}$  measured for adhesion loss. It is also equivalent to the  $67 \text{ kJ mol}^{-1}$  reported by Gledhill and Kinloch<sup>6</sup> for the formation of magnetite in bonds to cold rolled steel. Finally, it is interesting to note that the activation energy of  $68.7 \text{ kJ mol}^{-1}$  quite close to the  $70.3 \text{ kJ mol}^{-1}$  difference in standard enthalpies of formation for  $\text{ZnO}$  and  $\text{Zn(OH)}_2$ .<sup>11</sup> Since the surface originally consists of a substantial oxide layer,<sup>2</sup> this activation energy could be a direct reflection of the transformation of the oxide to the hydroxide.

#### The mechanism of adhesion loss

It is clear from a comparison of the activation energies listed in Table III that the rate limiting step in adhesion loss for steel substrates is the diffusion of water into the epoxy adhesive, since the activation energy for adhesion loss and that for moisture diffusion are equal, and both are significantly less than the activation energy for formation of corrosion product in the bond area. This accords with the conclusions of Gledhill and Kinloch,<sup>6</sup> although these authors did not measure the diffusion coefficient for their adhesive system.

For the same adhesive bonded to electroplated zinc, on the other hand, the activation energy for adhesion loss is essentially equal to the activation energy for

TABLE III  
Activation energies ( $\text{kJ mol}^{-1}$ ) for various processes

Process	Activation energy
Moisture diffusion	49.6 ( $\pm 1.8$ )
Adhesion loss, cold rolled steel	49.0 ( $\pm 3.4$ )
Adhesion loss, electroplated zinc	71.0 ( $\pm 7.4$ )
Corrosion, cold rolled steel	67 <sup>a</sup>
Corrosion, electroplated zinc	68.7 ( $\pm 5.3$ )

<sup>a</sup> Reference 6.

formation of corrosion product in the bond. Both of these values are significantly higher than that for moisture diffusion into the adhesive. Thus, bond strength loss is controlled by corrosion of the electroplated zinc layer, rather than by diffusion of moisture.

### CONCLUDING REMARKS

Since moisture diffusion into the adhesive is the rate determining step for adhesion loss of bonds to cold rolled steel, degradation of bond strength can, in principle, be retarded by using adhesives which have low moisture diffusivities. If the activation energy is sufficiently increased at the same time, it is even conceivable that substrate corrosion could become the dominant factor. However, as long as the presence of water results in adhesion loss, i.e., the interface is thermodynamically unstable in a moist environment, this mechanism cannot be entirely eliminated. An alternative approach to enhancing moisture stability has been described which entails the application of a zinc phosphate conversion coating followed by an electrodeposition primer prior to bonding.<sup>7</sup> In this way, the stability of bonds to cold rolled steel substrates can be enhanced significantly, so that in effect the moisture-induced strength deterioration can be eliminated.<sup>7</sup>

The measured activation energies for adhesion loss, moisture diffusion, and substrate corrosion (Table III) clearly show that corrosion of the electrodeposited zinc layer is responsible for bond strength loss. In practice, for adhesively bonded zinc-coated steel, it is therefore essential to provide reliable protection to bond edges to retard the initiation of corrosion. A very effective means of doing this is also the application of a conversion coating together with an electrodeposited primer.

It may not be possible to prevent strength loss entirely in the ways discussed above, particularly for bonds which are subjected to stress and moisture simultaneously, as well as to aqueous electrolyte and thermal fluctuations, which are present under many service conditions. However, it is likely that a substantial increase in durability will accompany these measures.

Finally, since different types of zinc-coated materials are currently available commercially, it is also pointed out that adhesive bonds to hot-dipped substrates will in all likelihood be *more* susceptible to strength deterioration *via* substrate

corrosion than bonds to electroplated substrates. Due to segregation of trace elements at grain boundaries during the solidification of hot-dipped coatings, the bonding surfaces of hot dipped zinc substrates contain significant quantities of Al, Pb, and Mg.<sup>2</sup> Depending on their relative electrode potentials, these elements will either drive the corrosion of the zinc at an increased rate relative to the electroplated substrates, which are "pure" zinc, or they will corrode preferentially themselves, again contributing to enhanced interfacial corrosion.<sup>5</sup>

### Acknowledgements

The authors would like to acknowledge the scanning electron microscopy work of C. A. Wong, Analytical Chemistry Department, General Motors Research Laboratories.

### References

1. R. T. Foister and K. J. Schroeder, *J. Adhesion* **24**, 259 (1987).
2. R. T. Foister, *J. Adhesion* **24**, 279 (1987).
3. J. R. Arnold, SAE Publication 862009, in *Proceedings of the Automotive Corrosion Prevention Conference*, Society of Automotive Engineers, Inc., Warrendale, PA, December, 1986, pp. 21-29.
4. J. R. Arnold, Bethlehem Steel Research Department Publication, January, 1988.
5. S. Maeda, T. Asai, S. Fujii, Y. Nomura and A. Nomoto, *J. Adhesion Sci. Technol.* **2**, 271 (1988).
6. R. A. Gledhill and A. J. Kinloch, *J. Adhesion* **6**, 315 (1974).
7. R. T. Foister, R. K. Gray and P. A. Madsen, *J. Adhesion* **24**, 47 (1987).
8. J. A. Schroeder, P. A. Madsen and R. T. Foister, *Polymer* **28**, 929 (1987).
9. J. A. Comyn, in *Durability of Structural Adhesives*, A. J. Kinloch Ed. (Applied Science Publishers, London, 1983), p. 85.
10. J. A. Schroeder, General Motors Research Laboratories (Private Communication).
11. *CRC Handbook of Chemistry and Physics*, **61st Edition** (CRC Press, Inc., Boca Raton, FL, 1981), p. D-78.